

# Genotype-Phenotype Correlation for *TGFBI* Corneal Dystrophies Identifies p.(G623D) as a Novel Cause of Epithelial Basement Membrane Dystrophy

Cerys J. Evans,<sup>1</sup> Alice E. Davidson,<sup>1</sup> Nicole Carnt,<sup>2,3</sup> Karla E. Rojas López,<sup>1</sup> Neyme Veli,<sup>2</sup> Caroline M. Thaug,<sup>1,2</sup> Stephen J. Tuft,<sup>1,2</sup> and Alison J. Hardcastle<sup>1</sup>

<sup>1</sup>University College London (UCL), Institute of Ophthalmology, London, United Kingdom

<sup>2</sup>Moorfields Eye Hospital, London, United Kingdom

<sup>3</sup>Save Sight Institute, The University of Sydney, Sydney, New South Wales, Australia

Correspondence: Alison J. Hardcastle, UCL Institute of Ophthalmology, 11 - 43 Bath street, London, EC1V 9EL, UK; a.hardcastle@ucl.ac.uk; Stephen J. Tuft, Moorfields Eye Hospital, 162 City Road, London, EC1V 2PD, UK; stephen.tuft@moorfields.nhs.uk.

Submitted: April 26, 2016

Accepted: August 25, 2016

Citation: Evans CJ, Davidson AE, Carnt N, et al. Genotype-phenotype correlation for *TGFBI* corneal dystrophies identifies p.(G623D) as a novel cause of epithelial basement membrane dystrophy. *Invest Ophthalmol Vis Sci.* 2016;57:5407-5414. DOI:10.1167/iops.16-19818

**PURPOSE.** The majority of anterior corneal dystrophies are caused by dominant mutations in *TGFBI* (transforming growth factor  $\beta$ -induced) collectively known as the epithelial-stromal *TGFBI* dystrophies. Most cases of epithelial basement membrane dystrophy (EBMD) are thought to result from a degenerative (nongenetic) process; however, a minority of cases are associated with specific *TGFBI* mutations. We evaluated the spectrum of *TGFBI* mutations and associated phenotypes in a United Kingdom cohort with typical epithelial-stromal *TGFBI* dystrophies and an EBMD cohort.

**METHODS.** We recruited 68 probands with a clinical diagnosis of epithelial-stromal *TGFBI* dystrophy and 23 probands with bilateral EBMD. DNA was extracted from peripheral leukocytes, and *TGFBI* was bi-directly Sanger sequenced.

**RESULTS.** Nine *TGFBI* mutations were identified. The most common occurred at the mutation hot-spot residues R124 and R555 in 61 probands; these individuals had a genotype-phenotype correlation consistent with prior reports. Four probands with lattice corneal dystrophy carried a mutation in exon 14: p.(A620D), p.(V625D), and p.(H626R). We identified a p.(G623D) mutation in five probands, including two probands from the EBMD cohort. These subjects typically had an onset of severe recurrent corneal epithelial erosion in the fourth decade with mild diffuse or geographic subepithelial corneal opacities and only small anterior stromal lattice structures in older individuals. Symptoms of painful epithelial erosion improved markedly following phototherapeutic keratectomy.

**CONCLUSIONS.** There was a strong correlation between genotype and phenotype for the majority of *TGFBI* mutations. In this cohort, the p.(G623D) mutation caused a greater proportion of *TGFBI*-associated disease than anticipated, associated with variable phenotypes including individuals diagnosed with EBMD.

**Keywords:** *TGFBI*, corneal dystrophy, granular, lattice, Reis-Bücklers, Thiel-Behnke, epithelial basement membrane dystrophy

Corneal dystrophies are a group of clinically and genetically heterogeneous disorders that cause corneal opacity with impaired vision and painful recurrent erosions. Dominant mutations in *TGFBI* (transforming growth factor  $\beta$ -induced) cause a number of clinically distinct corneal dystrophies including Reis-Bücklers corneal dystrophy (RBCD), Thiel-Behnke corneal dystrophy (TBCD), lattice corneal dystrophy (LCD), and granular corneal dystrophy (GCD). These mutations lead to an accumulation of *TGFBI* in the epithelial and stromal layers of the cornea. *TGFBI* mutations affecting amino acid residues R124 and R555 are the most common and are typically associated with a characteristic phenotype across ethnically diverse populations.<sup>1,2</sup>

Reis-Bücklers corneal dystrophy and TBCD are anterior stromal dystrophies caused by the *TGFBI* mutations p.(R124L) and p.(R555Q), respectively.<sup>1,3</sup> Clinically, RBCD is associated with a geographic pattern of superficial corneal opacities, whereas TBCD has a honeycomb pattern; although it is not

always possible to use this difference to reliably distinguish between the two conditions. These dystrophies are characterized by a deposition of continuous protein fibers primarily in the subepithelium and Bowman's layer. Histologically, they can be distinguished using Masson's trichrome by positive staining of RBCD deposits, which is absent in TBCD. Deposits of straight, rod-like collagen fibers are observed in RBCD corneal tissue by electron microscopy, whereas TBCD is associated with curly fibers.<sup>4,5</sup>

Lattice corneal dystrophy is characterized by the deposition of amyloid, primarily in the stroma, that produces a clinical appearance of thin, branching refractile lattice lines. Histology reveals fusiform deposits scattered throughout the stroma, concentrated predominantly below Bowman's layer.<sup>5</sup> A range of LCD phenotypes have been described, which vary in the appearance of the lattice lines, the severity of diffuse stromal haze, and the age of onset. The classic LCD phenotype is associated with the *TGFBI* mutation p.(R124C), whereas a



number of mutations, located predominantly in exon 14, are responsible for the many phenotypic variants of LCD.<sup>6</sup>

Granular corneal dystrophy type 1 (GCD1) is characterized by granular “crumb-like” deep stromal opacities, whereas individuals with GCD type 2 (GCD2) predominantly have a superficial “snowflake” pattern of opacities.<sup>2</sup> In GCD1, histology demonstrates distinct hyaline deposits in the corneal stroma that stain positively with eosin and Masson’s trichrome, whereas GCD2 is also positive for the presence of amyloid.<sup>5</sup> Granular corneal dystrophy type 1 is caused by *TGFBI* mutation p.(R555W) or p.(R124S), whereas GCD2 is caused by the mutation p.(R124H).<sup>1</sup> This striking genotype–phenotype correlation for epithelial-stromal *TGFBI* dystrophies suggests that each mutation has a specific gain-of-function effect.

Individuals with epithelial basement membrane dystrophy (EBMD) have thickening and reduplication of the epithelial basement membrane that appear clinically as map, dot, fingerprint, or bleb-like changes.<sup>7</sup> These can also be associated with painful recurrent corneal erosions.<sup>8</sup> Epithelial basement membrane dystrophy is considered to be a degenerative (nongenetic) disorder in the majority of individuals<sup>9</sup>; however, two dominant *TGFBI* mutations (p.[L509R] and p.[R666S]) have been reported in 3 probands with EBMD.<sup>10</sup> Recently, *COL17A1* mutations have been identified as the cause of epithelial recurrent erosion dystrophy (ERED), although the cornea can initially appear normal in these individuals between erosion episodes, without stromal deposits.<sup>11</sup> Therefore, the clinical condition of recurrent corneal erosion is likely genetically heterogeneous, or degenerative in some instances.

Resequencing studies in a wide range of populations have, to date, identified over 60 *TGFBI* mutations that cause corneal dystrophy. In this study, we investigated the spectrum of *TGFBI* mutations present in a large multi-ethnic UK cohort with epithelial-stromal *TGFBI* dystrophies. We also screened *TGFBI* in an additional cohort of patients with a diagnosis of bilateral EBMD. We have correlated these genetic findings with the presenting clinical phenotype and identified a novel association of EBMD with the *TGFBI* p.(G623D) mutation.

## MATERIALS AND METHODS

### Patient Recruitment and Clinical Examination

This study adhered to the tenets of the Declaration of Helsinki and had research ethics committee approval (REC: 13/LO/1084). Patients and relatives, where available, with a clinical diagnosis of RBCD, TBCD, LCD, GCD, or EBMD were examined at Moorfields Eye Hospital by a clinician experienced in inherited and acquired corneal disease (SJT). Data collected included family history, medical history, age of onset, and previous ocular surgery (e.g., keratoplasty, phototherapeutic keratectomy). Affected individuals had photographic documentation of their corneal changes. Patients with EBMD were included if they were bilaterally affected with subepithelial lines, cysts, or geographic opacities without a history of prior traumatic corneal abrasion. For patients who had keratoplasties, histology was performed for confirmation of affected disease status.

### Histology

Corneal tissue submitted for examination following keratoplasty was processed and stained with hematoxylin and eosin (H&E), periodic acid Schiff (PAS), Masson’s trichrome, and Congo red by routine methods,<sup>12</sup> and then examined by light microscopy.

## Genetic Screening

DNA was extracted from peripheral blood leukocytes using standard methods. *TGFBI* exons previously identified to harbor mutations (exons 4, 11, 12, 13, 14, and 16) were initially amplified by PCR (Supplementary Table S1) and Sanger sequenced in all probands, using standard protocols. Individuals who were negative for mutations within these exons were subsequently Sanger sequenced for all remaining *TGFBI* coding exons (17 coding exons in total). Individuals in the EBMD cohort who were negative for mutations in *TGFBI* were subsequently screened for two known mutations in *COL17A1* that have been associated with ERED. Sequences were aligned and compared with the reference sequence using DNASTAR Lasergene package software (Version 8.0.2; DNASTAR, Inc., Madison, WI, USA). Variants were annotated according to the NM\_000358.2 transcript with +1 representing the start of translation. Minor allele frequency (MAF) was determined using the exome aggregation consortium (ExAC) database (available in the public domain at <http://exac.broadinstitute.org/>).<sup>13</sup> Pathogenicity prediction programs SIFT (available in the public domain at <http://sift.jcvi.org/>)<sup>14</sup> and Polyphen2 (available in the public domain at <http://genetics.bwh.harvard.edu/pph2/>)<sup>15</sup> were used to predict the likely pathogenicity of variants. Segregation of variants was undertaken if DNA samples were available from additional family members.

## RESULTS

### Patient Cohort

A total of 91 probands (F1–F91) were recruited to the study, with a total of 110 DNA samples obtained for extended pedigrees. Sixty-eight probands had a clinical diagnosis of an epithelial-stromal *TGFBI*-associated dystrophy (RBCD, TBCD, LCD, and GCD). The majority of these probands had a family history of corneal disease that was consistent with an autosomal dominant pattern of inheritance. The remaining 23 probands were diagnosed with bilateral EBMD. Three EBMD probands had a positive family history of the corneal disease, with symptoms in at least one first-degree relative (F70, F88, and F90).

All *TGFBI* mutations identified were predicted to be pathogenic by SIFT and Polyphen2, except p.(R555Q), and have been previously identified as causing an epithelial-stromal *TGFBI* dystrophy. The majority were absent from the ExAC database with the exception of p.(R124C), present at a frequency of 0.0000083, and p.(R124H), present at a frequency of 0.000058 (accessed April 2016).

### Mutations at Residues R124 and R555 Demonstrate Complete Genotype–Phenotype Correlation

The most common mutations in our corneal dystrophy cohort occurred at the two mutation hot-spot residues, R124 and R555 (Fig. 1A, Table). Six distinct mutations affecting these residues have been described, each of which correlates with a well-characterized clinical phenotype.<sup>1,2</sup> In our cohort, we identified five of these mutations; however, the reported GCD1-associated mutation p.(R124S) was absent (Figs. 1A, 1B).<sup>1–3</sup>

### Thiel-Behnke and Reis-Bücklers Corneal Dystrophy

The c.1664G>A; p.(R555Q) mutation, reported to be associated with TBCD, was identified in 20 unrelated probands, whereas the RBCD-associated mutation (c.371G>T; p.[R124L])

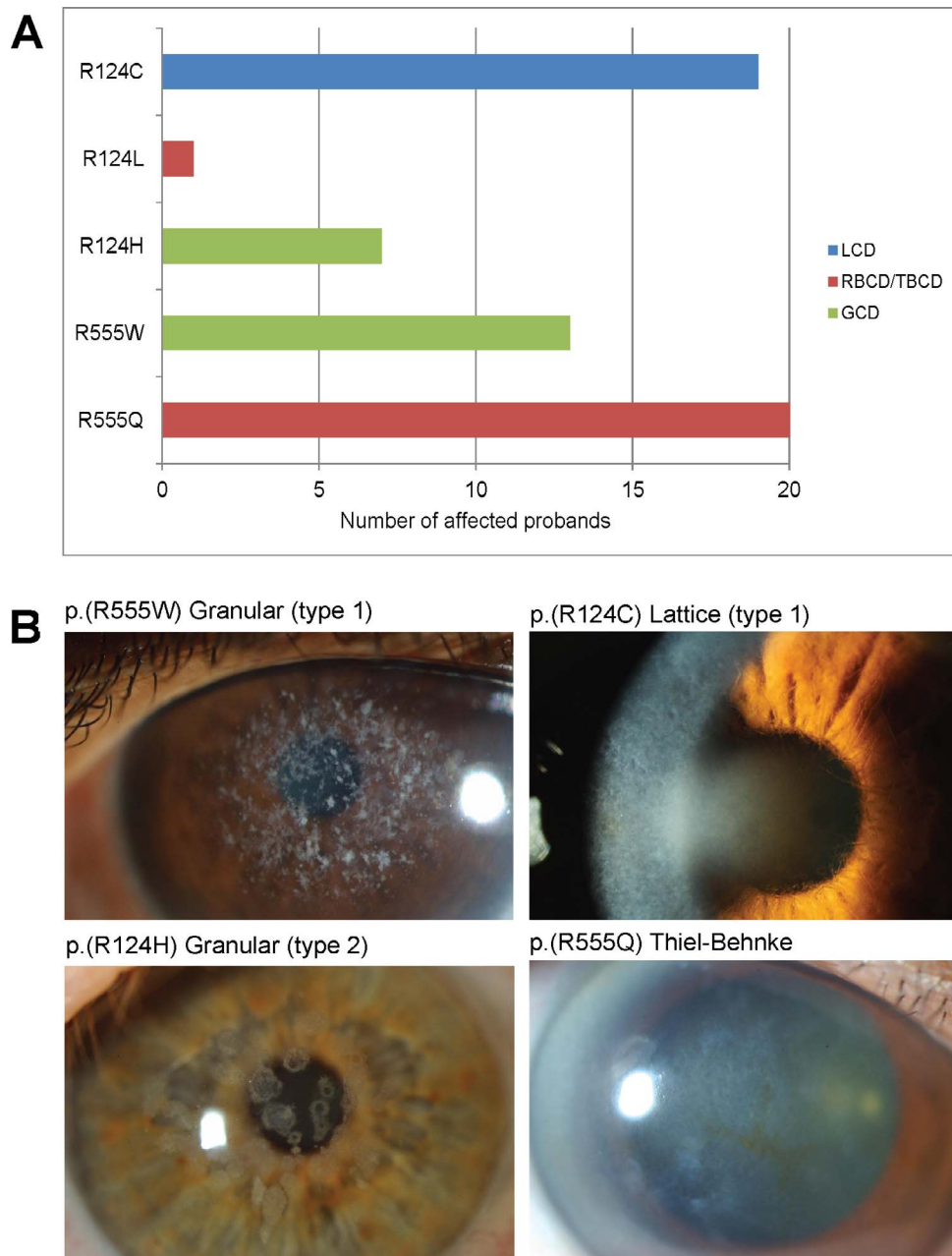


**FIGURE 1.** Genotype-phenotype correlation for mutations affecting mutation hot-spot residues R124 and R555. (A) Graph shows the clinical diagnosis and genotype of 61 probands harboring a *TGFBI* mutation affecting either amino acid R124 or R555. There is complete correlation between genotype and phenotype. (B) Where available, representative clinical images of the phenotype associated with mutations affecting R124 and R555 are shown.

was found in only one patient, demonstrating that TBCD is more prevalent in our patient population (Fig. 1A). All individuals in this group had anterior stromal opacity as previously described (Fig. 1B).

### Granular Corneal Dystrophy

Consistent with previous reports, individuals with GCD1 had predominantly deep granular opacities, while individuals with GCD2 had predominantly anterior stromal snowflake opacities (Fig. 1B). The GCD1 mutation c.1663C>T; p.(R555W) was more commonly detected (13 probands) than the GCD2 mutation c.371G>A; p.(R124H) (8 probands, Fig. 1A, Table).

### Lattice Corneal Dystrophy

Twenty-four probands had a phenotype consistent with LCD. The most common mutation was p.(R124C) found in 19 individuals (Fig. 1A, Table). All individuals carrying this mutation had branching refractile lines and stromal haze consistent with the classic lattice phenotype (Fig. 1B).

### Lattice Corneal Dystrophy Caused by Mutations in *TGFBI* Exon 14

Two probands (F18 and F84) had the mutation c.1877A>G; p.(H626R) (Fig. 2). In family F18, the proband's brother had asymmetric progression of disease with only minor changes in

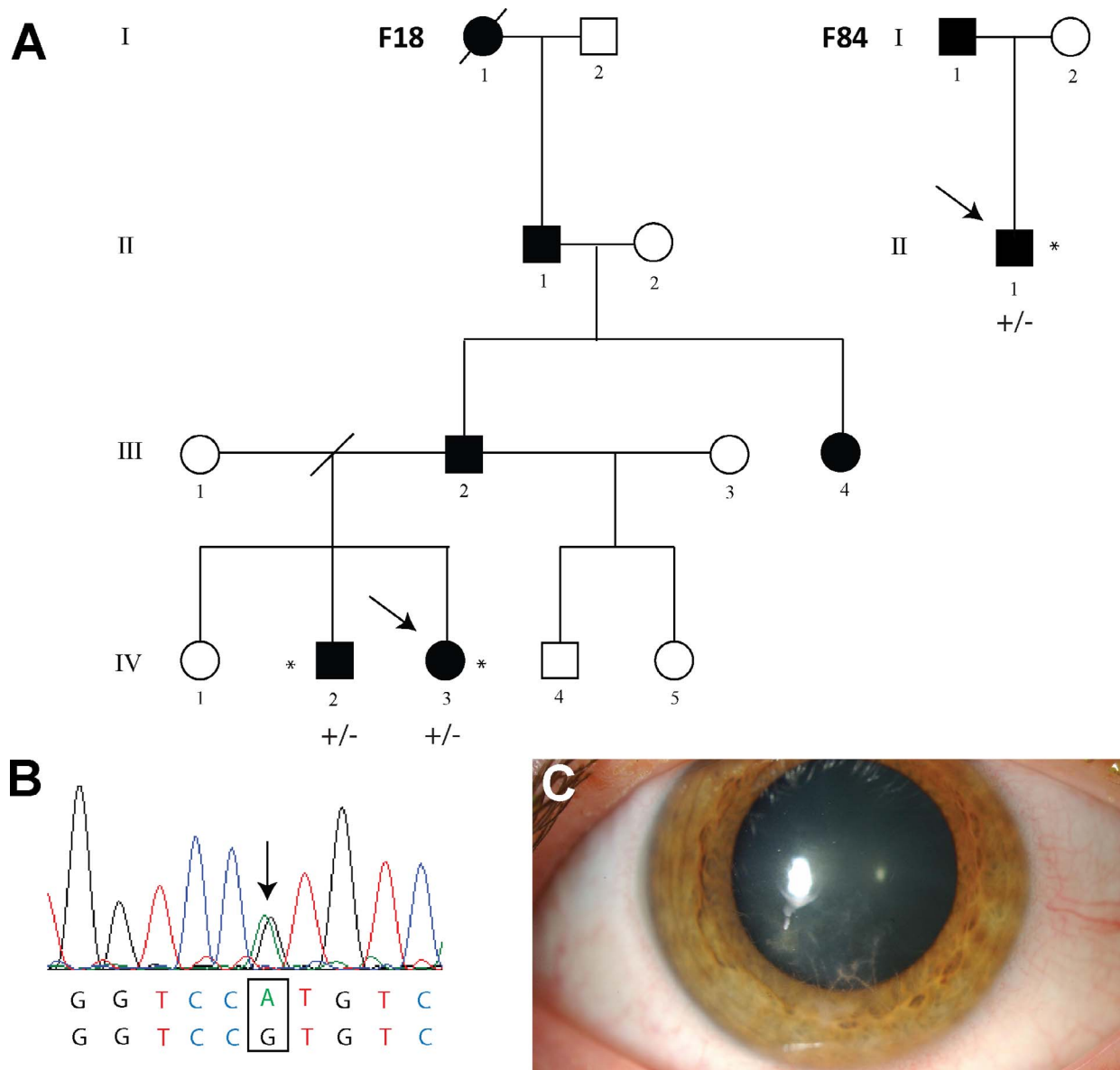


**FIGURE 2.** *TGFBI* mutation p.(H626R) identified in two families with LCD. (A) Pedigree showing inheritance of LCD in two unrelated families. The proband of the family is highlighted with an *arrow*. DNA samples were obtained from individuals indicated with a \* (B) Sequence electropherogram shows the presence of a heterozygous c.1877A>G; p.(H626R) mutation in exon 14. (C) Slit-lamp image shows minor lattice lines in one eye of IV:2 (F18).

one eye (Fig. 2C), consistent with previous reports of asymmetric disease associated with this mutation.<sup>6,16-18</sup> The clinical phenotype in both individuals was mild, with lattice lines predominantly below the visual axis.

Proband F14 was of South Asian ethnicity and was initially diagnosed with RBCD. *TGFBI* sequencing identified a heterozygous c.1874T>A; p.(V625D) mutation (Fig. 3B). The proband had a diffuse anterior stromal haze combined with small granular focal opacities. Lattice structures could not be visualized on biomicroscopy (Fig. 3C). Light microscopy demonstrated linear subepithelial deposition of amyloid as well as a few fusiform deposits within the superficial stroma. Masson's trichrome staining was negative, and the subepithelial fibrous sheet typical of RBCD and TBCD was absent, excluding both these diagnoses. The histologic diagnosis of lattice dystrophy was made (Fig. 3D).

Proband F60, of East Asian origin, had the c.1859C>A; p.(A620D) mutation. The clinical appearance was consistent with classic lattice dystrophy.

### Phenotypes Associated With the *TGFBI* Mutation p.(G623D)

Five probands were identified with the c.1868 G>A; p.(G623D) mutation, also located in exon 14 (Table). The clinical phenotype consisted of a diffuse or geographic pattern of superficial stromal opacity, with small refractile granules or lines. The phenotype was possibly modified by superficial corneal scar formation secondary to multiple epithelial erosions in both examined individuals from F70. All probands had a relatively late disease onset (fourth decade onward), with severe symptoms of recurrent corneal epithelial erosions and a

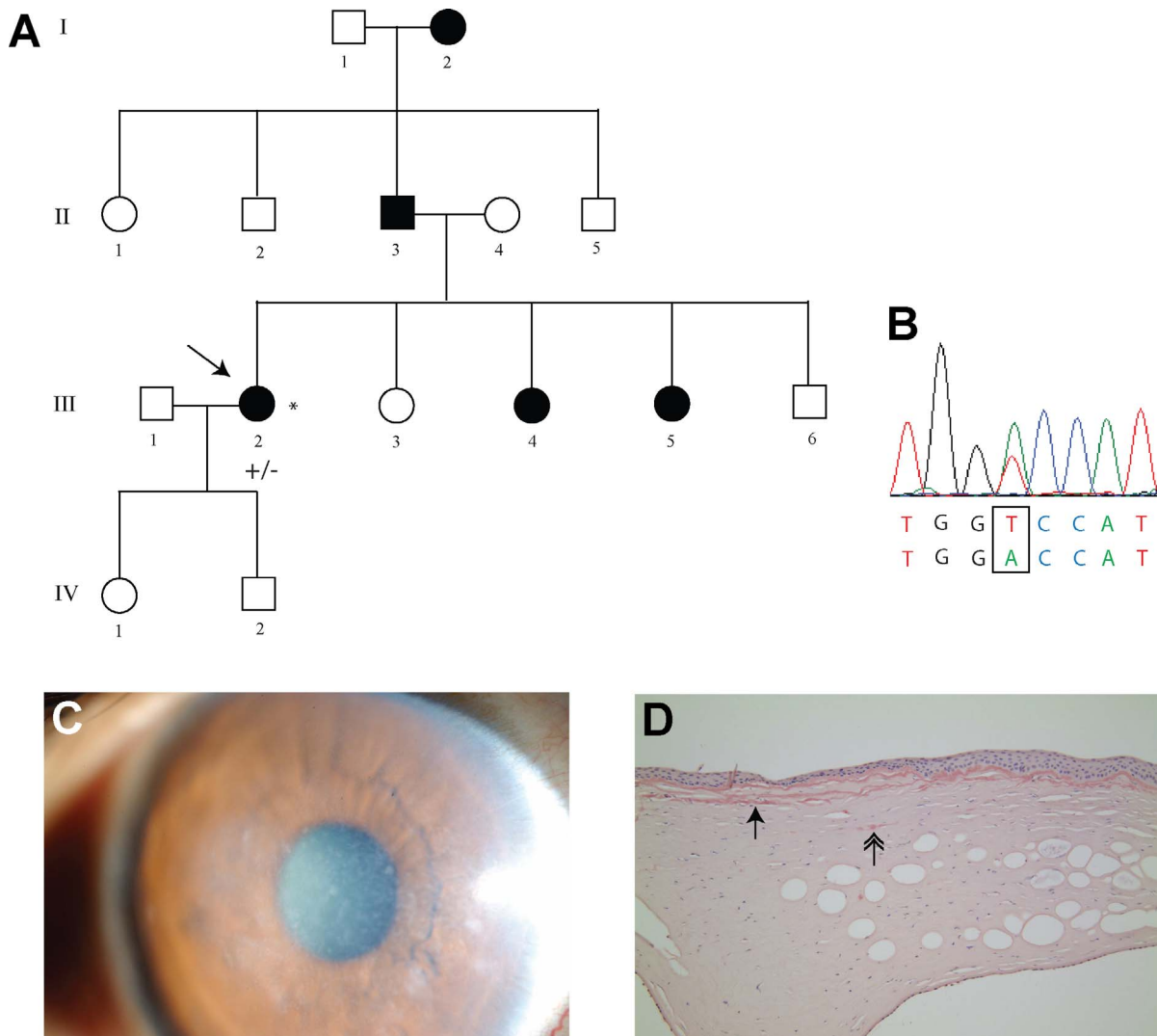


**FIGURE 3.** Inheritance of *TGFBI* p.(V625D) mutation associated with atypical LCD in proband F14. **(A)** Pedigree indicates an autosomal dominant inheritance of corneal dystrophy. **(B)** Sequencing *TGFBI* revealed the presence of a heterozygous c.1874T>A; p.(V625D) mutation in exon 14. **(C)** Slit-lamp image shows diffuse anterior stromal haze combined with small granular focal opacities. **(D)** Histologic sample demonstrates amyloid predominantly located near Bowman's layer (*arrow*) with a few stromal deposits (*doubled-headed arrow*), resulting in a diagnosis of LCD.

delay before a diagnosis of corneal dystrophy was considered. There had been diagnostic uncertainty in this cohort, with a diagnosis of LCD in one proband (F51), RBCD/TBCD in two probands (F21, F46), and EBMD in two probands (F59 and F70).

Proband F51 had late onset of severe recurrent corneal epithelial erosion in his sixties. There was a diffuse axial anterior stromal haze with small lattice structures resulting in a clinical diagnosis of LCD. The symptoms from erosion settled following laser phototherapeutic keratectomy (PTK) (Fig. 4A).

Proband F21 had been managed for several years for presumed bilateral herpes simplex keratitis before a diagnosis of RBCD/TBCD was considered. There was a geographic pattern of subepithelial haze and tiny granular structures (Fig. 4B). Her symptoms greatly reduced following laser PTK. Similarly, F46 had a diffuse subepithelial haze and small refractile structures (Fig. 4C). She had initially been managed for EBMD before a diagnosis of RBCD was considered.

Proband F59 had elevated serpiginous superficial opacities of both corneas, possibly secondary to subepithelial scar formation, but without stromal granular or lattice structures

(Fig. 4F). His father was not clinically examined but had been previously diagnosed with dry eye disease. Proband F70 and his father both had a similar pattern of focal superficial stromal opacities without stromal deposits (Figs. 4D, 4E). Again, it was uncertain whether these changes were owing to primary disease or scarring from recurrent episodes of epithelial breakdown.

The remaining 21 probands diagnosed with EBMD were negative for potentially pathogenic changes in all *TGFBI* protein coding exons and negative for the two ERED-associated mutations (p.[Thr939Ile] and p.[Gly1052Gly]) in *COL17A1*.

**DISCUSSION**

Over 60 pathogenic *TGFBI* mutations have been described to date. However, in our large multi-ethnic cohort, we found only a limited spectrum of nine mutations responsible for *TGFBI*-associated disease (Table). The p.(R555Q), p.(R555W), and p.(R124C) mutations, causing TBCD, GCD1, and LCD, respectively, were the most common, which is consistent with a previous case series of 16 probands.<sup>19</sup> Of interest, in the great

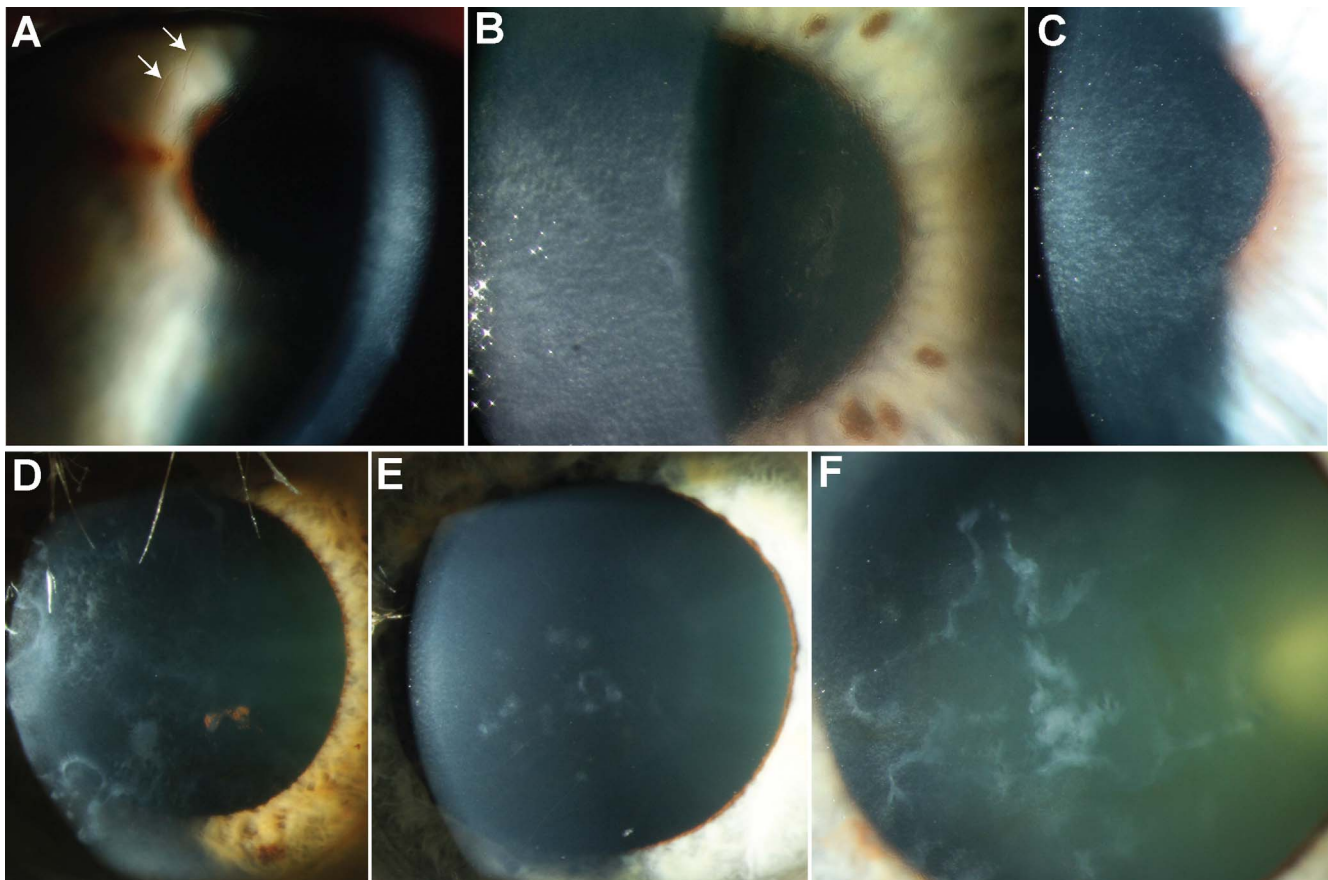


**FIGURE 4.** Phenotypic spectrum of disease associated with the p.(G623D) mutation. Clinical phenotype in five probands with the p.(G623D) mutation ranged from lattice lines in F51 (arrows) (A), opacities located at Bowman's layer in F21 (B) and F46 (C), and changes of the epithelial basement membrane in F70 (D, son of the proband F70; E, proband F70) and F59 (F).

majority of individuals with anterior stromal dystrophy we identified the p.(R555Q) mutation that has been associated with TBCD, with only a single proband carrying the p.(R124L) RBCD-associated mutation.

There were three mutations in this cohort that caused LCD in addition to the common hot-spot change for this condition. The p.(H626R) change, that we identified in two probands, is the most common LCD-associated mutation in Mexican<sup>20</sup> and Vietnamese<sup>16</sup> populations. The reported phenotype is described as atypical, with fewer, thicker lattice lines and a late onset compared with classic LCD.<sup>16</sup> This was consistent with the mild disease observed in family F18. The c.1874T>A; p.(V625D) mutation has been previously reported in one Chinese family with LCD; however, in this family, lattice lines were observed in the proband but not in his affected mother.<sup>21</sup> Histology confirmed the diagnosis of LCD in our proband with this mutation. The c.1859C>A; p.(A620D) mutation, identified in our proband of South Asian ethnicity, has also been previously reported in a Chinese patient.<sup>22</sup>

When we included the EBMD cohort, five unrelated probands harbored the p.(G623D) mutation. This mutation is therefore more prevalent in the United Kingdom population than previously recognized, and it accounts for a substantial proportion of the disease burden. The p.(G623D) mutation has been identified in patients from Filipino, European, and Chinese populations; therefore, it likely represents a mutation hot spot rather than an inherited founder mutation.<sup>3,23-26</sup>

Although the genotype-phenotype correlation for most *TGFBI* mutations is generally consistent, individuals with the p.(G623D) mutation had a range of clinical signs leading to

clinical diagnoses of RBCD/TBCD, LCD, or EBMD and, in some cases, had been previously misdiagnosed with bilateral herpes simplex keratitis or dry eye disease. It is probable that studies that do not consider a diagnosis of epithelial-stromal *TGFBI* dystrophy in patients with EBMD or other chronic ocular surface diseases will underestimate the prevalence of this mutation. Six other families carrying the p.(G623D) mutation have been described previously.<sup>3,23-26</sup> The most common phenotype is a geographic pattern of opacities at Bowman's layer, consistent with RBCD,<sup>23</sup> although some individuals also have the stromal lattice lines of LCD.<sup>26</sup> The majority of families described have similar clinical features within the affected family,<sup>27</sup> although some have intrafamilial variation.<sup>24</sup> The phenotypic variability associated with p.(G623D) may be the result of environmental or genetic modifiers of this mutation, secondary corneal scarring (Salzmann degeneration), or the accumulation of amyloid with age to form lattice lines in older individuals.

The histology of corneal tissue from individuals with the p.(G623D) mutation is also variable. One patient with clinical features of RBCD had opacities that were negative for PAS, Masson's trichrome, and Congo Red.<sup>23</sup> In another family with the p.(G623D) mutation, five corneal buttons were analyzed from three affected siblings with superficial opacities similar to Salzmann's nodular degeneration. These were positive for amyloid in Bowman's layer and the stroma.<sup>24</sup> Three other probands with map-like opacities and lattice lines also had tissue that stained positive for amyloid.<sup>25</sup>

The different pathogenic mutations located in the fourth fasciclin-1 (FAS-1) domain of the protein (Fig. 5), result in

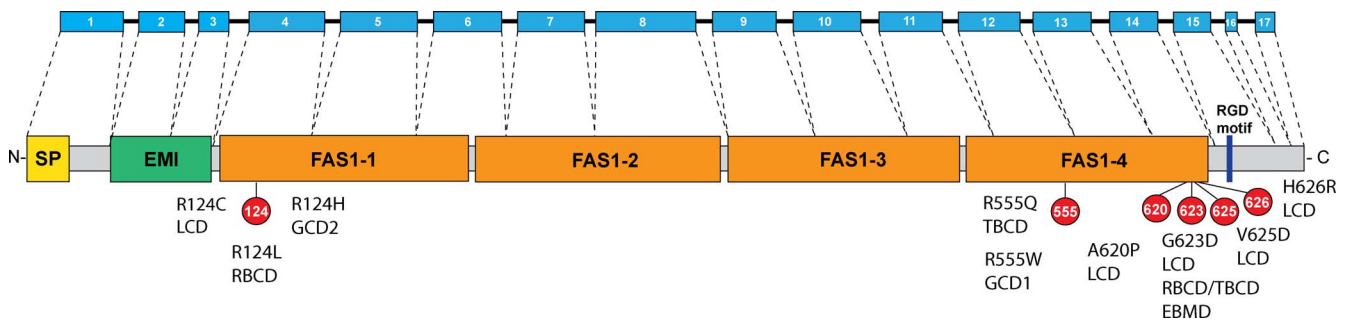


**FIGURE 5.** Diagrammatic representation of *TGFBI* gene and protein structure showing position of mutations detected and associated phenotype. *TGFBI* protein structure consists of an N-terminal signal peptide (SP) and N-terminal cysteine-rich (EMI) domain, followed by four fasciclin-1 (FAS-1) domains. RGD (Arg-Gly-Asp) motif is a potential integrin binding site. Exons are drawn to scale; introns are not drawn to scale but are included to demonstrate exon-intron boundaries. Transcript shown is NM\_000358.

specific physiochemical differences in the *TGFBI* protein, which may provide an insight into the diverse clinical phenotypes observed. The p.(R555W) mutant protein, associated with a GCD1 phenotype, has increased thermodynamic stability and is more resistant to proteolytic digestion than the wild-type protein. Conversely, the p.(A546T) protein (associated with LCD) has reduced stability and is more prone to proteolytic digestion relative to the wild-type protein.<sup>28,29</sup> The reduction of thermodynamic stability exposes a “fibril-core” (Y571-R588), which is released by proteolytic cleavage. Once released, these peptides form amyloid fibrils, which subsequently aggregate.<sup>30</sup> Given the clinical and histologic variability associated with the p.(G623D) mutation, it would be interesting to further investigate the mutant protein to determine its thermodynamic stability and aggregation propensity.

A previous study that screened *TGFBI* in a cohort of EBMD patients estimated that approximately 10% of these individuals have mutations in *TGFBI*.<sup>10</sup> This is consistent with our finding that p.(G623D) was present in 9% of the EBMD cohort; although neither of the two previously reported *TGFBI* mutations (p.[L509R] and p.[R666S]) were observed. Genetic testing is rarely performed for individuals with EBMD, as the basis for disease is thought to be degenerative. However, our results demonstrate that a reevaluation of a diagnosis of EBMD is warranted in some patients, particularly where there is a family history of corneal disease, when screening for *TGFBI* may be informative.

**TABLE.** Summary of 91 Unrelated Affected Probands in the Study Cohorts\*

Clinical Diagnosis	N (%)	<i>TGFBI</i> Mutations (N)
Lattice corneal dystrophy	24 (26%)	p.(R124C) (19) p.(V625D) (1) p.(H626R) (2) p.(A620D) (1) p.(G623D) (1)
Granular corneal dystrophy 1	21 (23%)	p.(R555W) (13)
Granular corneal dystrophy 2		p.(R124H) (8)
Thiel-Behnke/Reis-Bücklers corneal dystrophy	23 (25%)	p.(R555Q) (20) p.(R124L) (1) p.(G623D) (2)
Epithelial basement membrane dystrophy	23 (25%)	p.(G623D) (2) Negative (21)
Total	91	

\* Thiel-Behnke and Reis-Bücklers corneal dystrophy are grouped because histology (Masson’s trichrome staining) is required to reliably distinguish between the two conditions.

Identification of the p.(G623D) mutation in the EBMD cohort has important implications for clinical management and counseling for patients and their families, especially considering that in patients carrying this mutation, the symptoms of painful epithelial erosion improved markedly following PTK. There are also implications for patients with *TGFBI* dystrophies if they undergo LASIK.<sup>31</sup> Following photorefractive keratectomy (PRK) and LASIK surgery, an increase in stromal deposits and loss of visual acuity has been reported in several GCD2 patients carrying the *TGFBI* p.(R124H) mutation. Histology showed increased *TGFBI* hyaline deposits, particularly at the margin of the LASIK flap and in the stromal interface.<sup>32-34</sup> This may be owing to an upregulation of TGF-β1 expression by stromal fibroblasts after injury, which is part of the normal corneal wound healing response.<sup>35</sup>

The etiology of disease in the remaining EBMD patients in our cohort, including two probands with a family history of corneal erosions, who were negative for a mutation in *TGFBI* and for the two reported *COL17A1* mutations, is unknown. The relative contribution of alternative mutations in *COL17A1*, mutations in other as yet undiscovered gene(s), or corneal degeneration in this patient group remains to be elucidated.

**Acknowledgments**

The authors thank all the families for participating in this research, and Beverley Scott and Naushin Waseem for DNA extraction.

Presented in part at the annual meeting of the Association for Research in Vision and Ophthalmology, Seattle, WA, USA, May 2016.

Supported by Fight for Sight, Moorfields Eye Charity, Moorfields Special Trustees, Lanvern Foundation, Rosetrees Trust, and the National Institute for Health Research (NIHR) Biomedical Research Centre based at Moorfields Eye Hospital National Health Service (NHS) Foundation Trust and University College London (UCL) Institute of Ophthalmology.

Disclosure: **C.J. Evans**, None; **A.E. Davidson**, None; **N. Carnt**, None; **K.E. Rojas López**, None; **N. Veli**, None; **C.M. Thuang**, None; **S.J. Tuft**, None; **A.J. Hardcastle**, None

**References**

- Munier FL, Korvatska E, Djemai A, et al. Kerato-epithelin mutations in four 5q31-linked corneal dystrophies. *Nat Genet.* 1997;15:247-251.
- Stewart HS, Ridgway AE, Dixon MJ, Bonshek R, Parveen R, Black G. Heterogeneity in granular corneal dystrophy: identification of three causative mutations in the *TGFBI* (BIGH3) gene-lessons for corneal amyloidogenesis. *Hum Mutat.* 1999;14:126-132.

3. Munier FL, Frueh BE, Othenin-Girard P, et al. BIGH3 mutation spectrum in corneal dystrophies. *Invest Ophthalmol Vis Sci.* 2002;43:949-954.
4. Kuchle M, Green WR, Volcker HE, Barraquer J. Reevaluation of corneal dystrophies of Bowman's layer and the anterior stroma (Reis-Bucklers and Thiel-Behnke types): a light and electron microscopic study of eight corneas and a review of the literature. *Cornea.* 1995;14:333-354.
5. Dighiero P, Niel F, Ellies P, et al. Histologic phenotype-genotype correlation of corneal dystrophies associated with eight distinct mutations in the TGFB1 gene. *Ophthalmology.* 2001;108:818-823.
6. Schmitt-Bernard CF, Guittard C, Arnaud B, et al. BIGH3 exon 14 mutations lead to intermediate type I/IIIA of lattice corneal dystrophies. *Invest Ophthalmol Vis Sci.* 2000;41:1302-1308.
7. Laibson PR. Microcystic corneal dystrophy. *Trans Am Ophthalmol Soc.* 1976;74:488-531.
8. Reidy JJ, Paulus MP, Gona S. Recurrent erosions of the cornea: epidemiology and treatment. *Cornea.* 2000;19:767-771.
9. Weiss JS, Moller HU, Aldave AJ, et al. IC3D classification of corneal dystrophies—edition 2. *Cornea.* 2015;34:117-159.
10. Boutboul S, Black GC, Moore JE, et al. A subset of patients with epithelial basement membrane corneal dystrophy have mutations in TGFB1/BIGH3. *Hum Mutat.* 2006;27:553-557.
11. Jonsson F, Bystrom B, Davidson AE, et al. Mutations in collagen, type XVII, alpha 1 (COL17A1) cause epithelial recurrent erosion dystrophy (ERED). *Hum Mutat.* 2015;36:463-473.
12. Suvarna KS, Layton C, Bancroft JD. Bancroft's Theory and Practice of Histological Techniques. London: Churchill Livingstone; 2013.
13. Lek M, Karczewski K, Minikel E, et al. Analysis of protein-coding genetic variation in 60,706 humans. *Nature.* 2016;536:285-291.
14. Ng PC, Henikoff S. SIFT: predicting amino acid changes that affect protein function. *Nucleic Acids Res.* 2003;31:3812-3814.
15. Adzhubei IA, Schmidt S, Peshkin L, et al. A method and server for predicting damaging missense mutations. *Nat Methods.* 2010;7:248-249.
16. Chau HM, Ha NT, Cung LX, et al. H626R and R124C mutations of the TGFB1 (BIGH3) gene caused lattice corneal dystrophy in Vietnamese people. *Br J Ophthalmol.* 2003;87:686-689.
17. Schmitt-Bernard CF, Schneider C, Argiles A. Clinical histopathologic, and ultrastructural characteristics of BIGH3(TGFB1) amyloid corneal dystrophies are supportive of the existence of a new type of LCD: the LCDi. *Cornea.* 2002;21:463-468.
18. Lai K, Reidy J, Bert B, Milman T. Spheroidal degeneration in H626R TGFB1 variant lattice dystrophy: a multimodality analysis. *Cornea.* 2014;33:726-732.
19. El-Ashry ME, Abd El-Aziz MM, Hardcastle AJ, Bhattacharya SS, Ebenezar ND. A clinical and molecular genetic study of autosomal-dominant stromal corneal dystrophy in British population. *Ophthalmic Res.* 2005;37:310-317.
20. Zenteno JC, Correa-Gomez V, Santacruz-Valdez C, Suarez-Sanchez R, Villanueva-Mendoza C. Clinical and genetic features of TGFB1-linked corneal dystrophies in Mexican population: description of novel mutations and novel genotype-phenotype correlations. *Exp Eye Res.* 2009;89:172-177.
21. Tian X, Fujiki K, Zhang Y, et al. A novel variant lattice corneal dystrophy caused by association of mutation (V625D) in TGFB1 gene. *Am J Ophthalmol.* 2007;144:473-475.
22. Lakshminarayanan R, Vithana EN, Chai SM, et al. A novel mutation in transforming growth factor-beta induced protein (TGFB1p) reveals secondary structure perturbation in lattice corneal dystrophy. *Br J Ophthalmol.* 2011;95:1457-1462.
23. Afshari NA, Mullally JE, Afshari MA, et al. Survey of patients with granular, lattice, avellino, and Reis-Bucklers corneal dystrophies for mutations in the BIGH3 and gelsolin genes. *Arch Ophthalmol.* 2001;119:16-22.
24. Auw-Haedrich C, Agostini H, Clausen I, et al. A corneal dystrophy associated with transforming growth factor beta-induced Gly623Asp mutation an amyloidogenic phenotype. *Ophthalmology.* 2009;116:46-51.
25. Gruenauer-Kloevokorn C, Clausen I, Weidle E, et al. TGFB1 (BIGH3) gene mutations in German families: two novel mutations associated with unique clinical and histopathological findings. *Br J Ophthalmol.* 2009;93:932-937.
26. Aldave AJ, Rayner SA, King JA, Affeldt JA, Yellore VS. A unique corneal dystrophy of Bowman's layer and stroma associated with the Gly623Asp mutation in the transforming growth factor beta-induced (TGFB1) gene. *Ophthalmology.* 2005;112:1017-1022.
27. Li D, Qi Y, Wang L, Lin H, Zhou N, Zhao L. An atypical phenotype of Reis-Bucklers corneal dystrophy caused by the G623D mutation in TGFB1. *Mol Vis.* 2008;14:1298-1302.
28. Runager K, Basaiawmoit RV, Deva T, et al. Human phenotypically distinct TGFB1 corneal dystrophies are linked to the stability of the fourth FAS1 domain of TGFB1p. *J Biol Chem.* 2011;286:4951-4958.
29. Underhaug J, Koldso H, Runager K, et al. Mutation in transforming growth factor beta induced protein associated with granular corneal dystrophy type 1 reduces the proteolytic susceptibility through local structural stabilization. *Biochim Biophys Acta.* 2013;1834:2812-2822.
30. Sorensen CS, Runager K, Scavenius C, et al. Fibril core of transforming growth factor beta-induced protein (TGFB1p) facilitates aggregation of corneal TGFB1p. *Biochemistry.* 2015;54:2943-2956.
31. Woreta FA, Davis GW, Bower KS. LASIK and surface ablation in corneal dystrophies. *Surv Ophthalmol.* 2015;60:115-122.
32. Kim TI, Roh MI, Grossniklaus HE, et al. Deposits of transforming growth factor-beta-induced protein in granular corneal dystrophy type II after LASIK. *Cornea.* 2008;27:28-32.
33. Jun RM, Tchah H, Kim TI, et al. Avellino corneal dystrophy after LASIK. *Ophthalmology.* 2004;111:463-468.
34. Poulsen ET, Nielsen NS, Jensen MM, et al. LASIK surgery of granular corneal dystrophy type 2 patients leads to accumulation and differential proteolytic processing of transforming growth factor beta-induced protein (TGFB1p). *Proteomics.* 2016;16:539-543.
35. Song QH, Singh RP, Richardson TP, Nugent MA, Trinkaus-Randall V. Transforming growth factor-beta1 expression in cultured corneal fibroblasts in response to injury. *J Cell Biochem.* 2000;77:186-199.